Available online at www.sciencedirect.com

ScienceDirect

Ceramics International 39 (2013) 8979–8983

CERAMICS INTERNATIONAL

www.elsevier.com/locate/ceramint

Sintering and mechanical properties of MgO-doped nanocrystalline hydroxyapatite

C.Y. Tan[a], A. Yaghoubi[a], S. Ramesh[a,*], S. Adzila[a], J. Purbolaksono[a], M.A. Hassan[a], M.G. Kutty[b]

[a]*Department of Mechanical Engineering, Advanced Manufacturing and Material Processing (AMMP) Centre, University of Malaya, Kuala Lumpur, 50603 Malaysia*

[b]*Dental Research and Training Unit, Faculty of Dentistry, University of Malaya, Kuala Lumpur, 50603 Malaysia*

Received 25 March 2013; received in revised form 25 April 2013; accepted 25 April 2013
Available online 4 May 2013

Abstract

Hydroxyapatite (HA) has been extensively studied for its exceptional ability in promoting osseointegration as in bone graft substitute and biomimetic coating of prosthetic implants. However poor mechanical properties of HA, in particular its low fracture toughness, has made its widespread adaption in a number of biomedical applications challenging. Here we employ an optimized wet precipitation method to synthesize nanocrystalline HA with significantly improved mechanical properties. In addition doping by MgO is found to effectively suppress grain growth and enhance fracture toughness by nearly 50% while good densification and phase stability in all samples regardless of concentration of dopant are fully maintained. Microstructural analysis further suggests that the exceptionally superior mechanical properties can be explained by migration of MgO to grain boundaries where they transform the more common transgranular fracture into an intergranular mode. Our biodegradation tests also confirm that MgO-doped HA is indeed a suitable candidate for load bearing implants.

Keywords: C. Mechanical properties; Hydroxyapatite; Sinterability; Synthesis; Relative density

1. Introduction

Bone diminution especially in women can begin in early adulthood as part of the natural process of aging [1]. In fact frailty syndrome along with atherosclerosis has been among the most common public health issues since the late decades of the 20th century [2]. With accelerating osteoporosis and osteomalacia either in elderly people or in patients suffering from bone mineral deficiency, non-traumatic pathologic fractures may eventually develop into more severe conditions requiring a total replacement of the damaged bones. Currently most prosthetic implants are fabricated from titanium alloys due to their superior biocompatibility and enhanced corrosion resistance compared to stainless steels and cobalt-based alloys [3].

Addition of a layer of HA, the main inorganic constituent of natural bone, on titanium prostheses has been proven to not only improve osteogenesis [4] but provide early pain relief and durability [5], however, given the poor adhesion of such coatings to the metallic substrate [6] development of implants solely based on HA is highly desirable. These are particularly of interest for load bearing joint implants including those of hip and knee in which the HA particles from the worn coating have been shown to induce third-body wear and ultimately severe osteolysis [7]. While previous studies have tried to enhance the poor mechanical properties of HA by addition of carbon nanotubes [8], glass [9] or yttrium-stabilized zirconia (YSZ) [10], none of them has reported a significant increase in fracture toughness. Incorporation of large percentage of other ceramics such as Al_2O_3 and intermetallic compounds such as Ni_3Al on the other hand even though provides vast improvements over plain HA, pose question on biocompatibility of these heavily modified composites [11].

To mitigate these problems, here we develop a new approach to synthesize nanocrystalline HA with considerably better sinterability over commercially available HA. The phase composition and size of the grains were studied using powder X-ray diffraction (XRD) and scanning electron microscopy

*Corresponding author. Tel.: +603 7967 5204; fax: +603 7967 5317.
E-mail address: ramesh79@um.edu.my (S. Ramesh).

0272-8842/$ - see front matter © 2013 Elsevier Ltd and Techna Group S.r.l. All rights reserved.
http://dx.doi.org/10.1016/j.ceramint.2013.04.098

(SEM) for a large number of samples with 0.05 wt% to 1.0 wt% of MgO. Moreover data on fracture toughness, Vickers hardness and Young's modulus obtained through microindentation tests are presented for samples of different dopant concentration. The results indicate that an optimally doped HA can be toughened by as much as 50% through our method. We further propose a new model based on transformation of transgranular fracture into an intergranular mode to explain the significantly enhanced mechanical properties in our samples. With the already proven biocompatibility of MgO [12,13] we expect this work to help realize load bearing HA implants for biomedical applications.

2. Methods & materials

In the present work, 98% pure calcium hydroxide $Ca(OH)_2$ and orthophosphoric acid H_3PO_4 (85% purity, Merck) were used as starting precursors to produce HA following the chemical reaction (molar ratio of Ca/P=1.67):

$$10Ca(OH)_2+6H_3PO_4 \Rightarrow Ca_{10}(PO_4)_6(OH)_2+18H_2O \quad (1)$$

Aqueous H_3PO_4 solution was added drop wise (6–11 drops per second) into a magnetically stirring suspension of $Ca(OH)_2$ in distilled water. Throughout the titration process, the pH of the mixture was maintained at 10.5 by adding small amounts of ammonium (NH_3) or ammonium hydroxide (25% concentration, Sigma Aldrich). After the titration process stirring was continued for another 6 h after which the solution started to coagulate. The precipitate was then allowed to settle down overnight before filtration. The filtered precipitate was subsequently rinsed thoroughly by distilled water and then dried overnight in an oven at about 60 °C. The dried filtered cake was crushed and sieved to obtain a well-defined, highly crystalline HA powder.

For the doping experiment, the 99% pure magnesium oxide (MgO) powder was purchased from Merck. Different concentrations of MgO were added to nanocrystalline HA by dispersing the powders in 200 mLs of ethanol via ultrasonication at 28–34 kHz for a predetermined period. The mixture was then wet milled for 1 h with zirconia beads (3 mm in diameter) and ethanol as the milling media. The resulting slurry was dried at 60 °C in a standard box oven for 24 h prior to filtration. The dried filtered cake was then crushed and sieved to give ready to compact MgO-doped HA powders.

The as-prepared MgO-doped HA powders were uniaxially compacted under 1.3–2.5 MPa into discs (20 mm diameter × 5 mm thickness) and into rectangular bars (32 × 13 × 6) mm. The green compacts were subsequently cold isostatically pressed (CIP) under a pressure of 200 MPa (Riken, Seiki, Japan). The compacted green bulk samples were then sintered at different temperatures from 1000 °C to 1350 °C with an interval of 50 °C and a ramp rate of 2 °C/min (heating and cooling) as well as a soaking time of 2 h. Prior to testing, each sample was polished to 1 μm finish using silicon carbide (SiC) sandpapers of different grit sizes. Commercial HA samples from Merck and Sigma Aldrich were also prepared in the same manner for conduction of comparative tests.

Phase stability of samples was studied using XRD (Geiger-Flex, Rigaku Japan). Young's Moduli were determined via sonic resonance method (GrindoSonic: MK5 "Industrial", Belgium) while Vickers Hardness and fracture toughness tests were performed on a standard microindentation device (Matsuzawa, Japan). Finally relative density of samples was measured using water immersion technique (Mettler Toledo, Switzerland).

For biocompatibility studies, the specimens were immersed in separate and enclosed vials containing 20 mL of calcium and protein-free Hank's solution with a pH of 7.4 (see Table 1 for the detailed composition). The temperature was maintained at 36.5 °C ± 0.1 °C to simulate human's body. In order to examine the dissolution rate of the samples, the mass of the specimens were measured before and after immersion at selected periods of 1, 5, 10, 20 and 30 days. Prior to any measurement the specimens were washed carefully with distilled water to remove residual Hank's solution and then dried at room temperature. In addition the HA phase stability was further evaluated by XRD after exposure to Hank's solution and no signs of deterioration were observed.

3. Results and discussion

The initial HA nanopowder was prepared through an optimized wet precipitation method based on reaction of phosphate and calcium ions in a titrated aqueous solution under controlled alkaline pH. Morphology of the as-synthesized product as observed using transmission electron microscopy (TEM) resembles columns of various lengths with an average diameter of 20 nm. Addition of any amount of MgO up to 1.0 wt% does not appear to disrupt this crystalline order as evident from the XRD data (Fig. 1) obtained from a variety of doped and undoped samples. Besides no diffraction peaks associated with intermediate apatites or secondary phases of α- and β-TCP (Tricalcium Phosphate) can be detected which further suggests the influence of MgO doping, if any, is largely limited to nucleation attributes during sintering. This change of behaviour in fact can be readily noticed in SEM micrographs of Fig. 2. The average grain size measured for undoped HA is about 10.5 μm at a relatively high sintering temperature of 1350 °C whereas for 0.3 wt% and 1.0 wt% of MgO, the average grain size drops steeply to 8 μm and 3.5 μm respectively. Due to superior sinterability of nanocrystalline HA, at lower temperatures, finer

Table 1
Composition of Hank's balanced salt solution used for biodegradation test.

Constituent	KCl	KH_2PO_4	NaCl	$NaHCO_3$	$Na_2HPO_4.2H_2O$
gram/litre	0.4	0.06	8	0.35	0.06

grain sizes on the order of ~300 nm for undoped HA and ~150 nm for 1 wt% MgO-doped HA were obtained.

As presented in Fig. 3(a), doping of plain nanocrystalline HA samples with different concentrations of MgO noticeably enhances fracture toughness with the highest value recorded at 1.48 ± 0.17 MPa $m^{1/2}$ for 1.0 wt% MgO-doped HA samples sintered at 1150 °C. Such an explicit change in properties after doping can equally be dependent upon the properties of undoped nanocrystalline HA which also demonstrates higher values on the order of 1.08 ± 0.05 MPa $m^{1/2}$, a nearly 10% improvement over commercially available powders. Furthermore other mechanical properties such as Vickers hardness and Young's modulus both have greatly increased in nanocrystalline HA and addition of MgO has more or less maintained or slightly reinforced this attribute. This is unlike any commercial powder which due to incorporation of secondary phases and calcium oxide may have highly fluctuating properties. For instance Vickers hardness in a typical HA sample may be about 1.17 ± 0.073 GPa at a sintering temperature of 1000 °C whereas for a sample sintered at 1250 °C, this value can be as

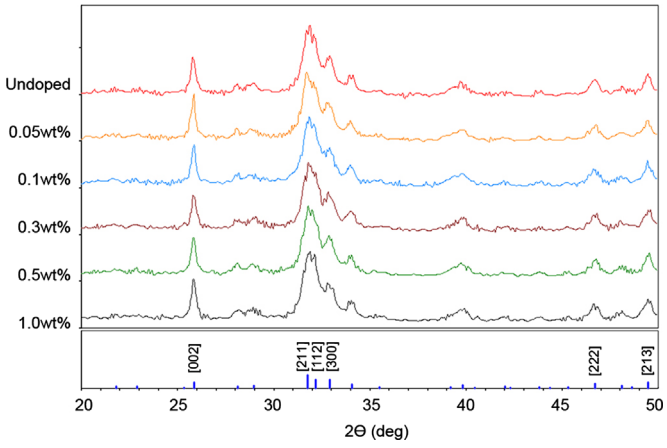

Fig. 1. XRD profiles of undoped and doped HA samples. No signs of secondary phases or calcium oxide can be detected. A set of low-intensity peaks from 36° to 37° are characteristic fingerprints of a monoclinic HA which unlike its hexagonal counterpart has an ordered arrangement of hydroxyl ions [14]. The large FWHM (full width at half maximum) in majority of peaks can be attributed to broadening due to small size of the nanocrystalline HA.

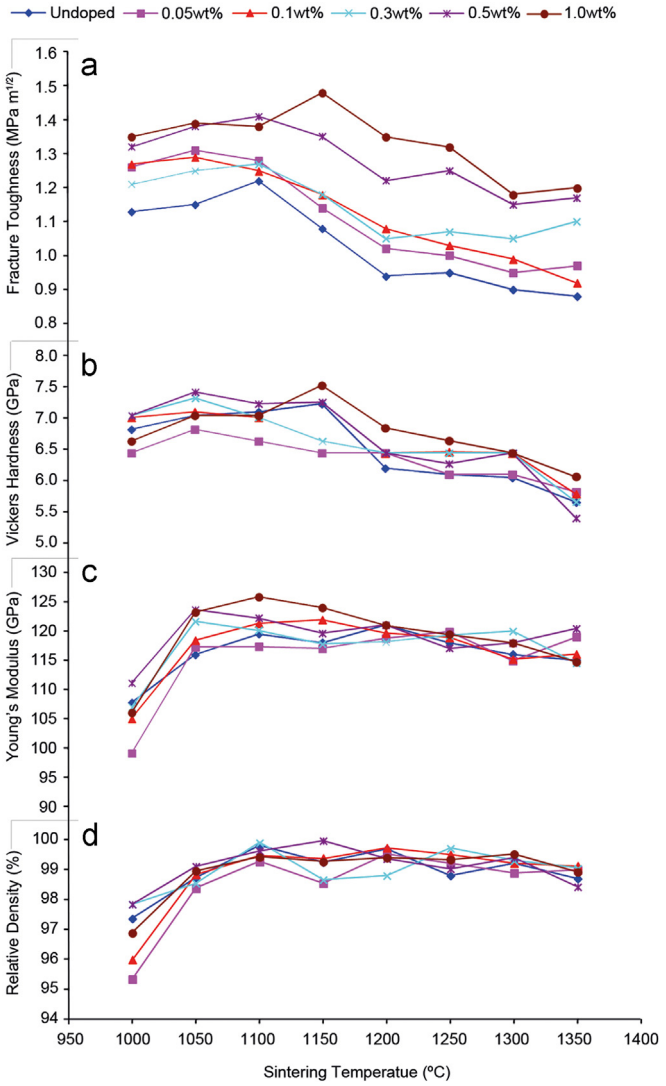

Fig. 3. Mechanical properties and sinterability of undoped and doped nanocrystalline HA. While there is a significant increase in fracture toughness for MgO-doped samples, Young's modulus and Vickers hardness have remained relatively constant regardless of dopant's concentration. All mechanical properties as well as densification behaviour have remarkably improved in nanocrystalline HA synthesized via optimized wet precipitation compared to commercially available powders (Merck and Sigma Aldrich). Densification over 95% at only 1000 °C allows formation of ultrafine grains in polycrystalline HA with an average size of 150 nm.

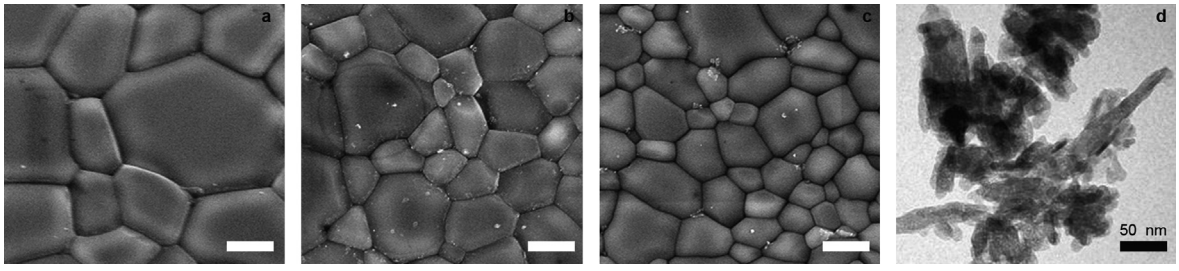

Fig. 2. Effect of MgO doping on microstructure of polycrystalline bulk HA. The average grain size for undoped HA sintered at 1350 °C is about 10.5 μm and addition of any amount of MgO, here 0.3 wt% and 1.0 wt% in (b) and (c) respectively effectively suppresses grain growth. Ultrafine grains with an average size of 150 nm can be obtained at lower sintering temperatures. A TEM micrograph (d) of the as-synthesized nanocrystalline HA is also presented. All scale bars are 5 μm unless indicated otherwise.

large as 6.08 ± 0.28 GPa [15]. On the contrary our nanocrystalline HA even at considerably low sintering temperatures exhibits exceptionally stable measurements of about 6.0 to 7.52 GPa. A similar analogy is applicable to Young's modulus for which the reported values can be anywhere from 34.5 GPa to 117 GPa [16] whereas in our samples the measurements are very stable as shown in Fig. 3(c). At a sintering temperature of 1100 °C, a value of 125.9 GPa was achieved for 1.0 wt% MgO compared to a Young's modulus of 119.5 GPa for the undoped HA.

As earlier mentioned the biocompatibility of MgO has been previously studied both in vivo and in vitro and no signs of cytotoxicity and deterioration of osseointegration with biological apatites have been reported thus far [12,13]. However considering the prominent effect of doping on microstructures in our samples, especially with possible concentration of MgO near the grain boundaries, further study on durability of doped HA samples in a simulated biological environment can be helpful.

Corrosion behaviour of HA bioceramics having different dopant concentrations was studied by measuring dissolution rate after total immersion for up to 30 days in calcium and protein free Hank's balanced salt solution (HBSS) at a constant temperature of 36.5 °C ± 0.1 °C (equivalent o body temperature). The mass loss for undoped HA was found to be ~0.3 mg/g after 30 days while for 1.0 wt% MgO-doped this value was in fact slightly less at ~0.2 mg/g.

In addition XRD results performed after biodegradation tests show no sign of structural change in both doped and undoped samples. This is consistent with a number of our previous studies which suggested secondary phases and calcium oxide may be the main reason behind rapid dissolution. In our case addition of greater concentrations of MgO (~5 wt%) seems to even contribute to a better biochemical stability making MgO-doped HA ideal for any potential clinical application. Such a characteristic is unlike many other dopants such as strontium for which a mass loss of more than 2.5 mg/g after only 2 days of immersion has been reported [17].

Kinetics of crystal nucleation and eventually formation of grains in polycrystalline bulk samples is a determining factor in successful doping of materials. In general particles which possess superior crystallinity show better sinterability at lower temperatures and in turn prevent growth of larger grains and poor mechanical properties. Incorporation of dopants into a sample with large concentration of imperfections such as those associated with carbonate [18] or calcium oxide as in sol–gel derived HA [19] may yield undesirable inhomogeneities rather than improved properties. Preparation of high quality nanocrystalline HA is therefore among the most crucial steps in enhancing the properties of bulk polycrystalline HA.

It is clear that addition of MgO can effectively suppress grain growth in high quality HA samples and thus enhance their mechanical properties significantly. The resulting ultrafine grains then are perhaps the most prominent factor that contribute to the high fracture toughness of MgO-doped HA as suggested by Hall-Petch equation, $\sigma_f = \sigma_o + kd^{-1/2}$, where σ_f is the fracture strength, d is the grain size, k and σ_o are constants. Further investigation on the role of MgO in promoting superior mechanical properties in HA can be based upon work fracture of toughness calculated as $G_{IC} = (K_{IC})^2/E$. Here K_{IC} is the fracture toughness and E is Young's modulus. The calculated G_{IC} for 1.0 wt% MgO-doped samples varies from 12 to 18 J/m^2 depending on sintering temperature while this value for undoped HA is within the considerably lower range of 6–12 J/m^2.

We can postulate from Fig. 3 that while fracture toughness has drastically improved in MgO-doped samples, the effect of doping on Vickers hardness or Young's modulus is minimal if not non-existent. This might be related to how fracture develops at nanoscale in doped nanocrystalline samples. Fig. 4 depicts a common diamond-shaped indent from Vickers microindentation test on a MgO-doped HA sample. Nanocracks initiated from the indent's edge in doped samples propagate on a zigzag path implying an intergranular fracture mode whereas in undoped HA, the grain boundaries appear to be more resistant compared to the grain's interior and therefore favour a transgranular fracture. We suggest that a transformation from transgranular to intergranular mode originates from migration of MgO impurities to regions near the grain boundaries where they give rise to an effective damping system at nanoscale responsible for controlling nanocracks growth. This implication is consistent with the fact that unlike fracture toughness, hardness and stiffness were not influenced noticeably by MgO doping. Despite this relative separation between HA and MgO dopant, the unusually good densification properties of nanocrystalline HA are fully maintained in doped samples as evidenced by relative density measurements presented in Fig. 3(d). Unlike any type of synthetic HA reported before [20], our samples regardless of concentration

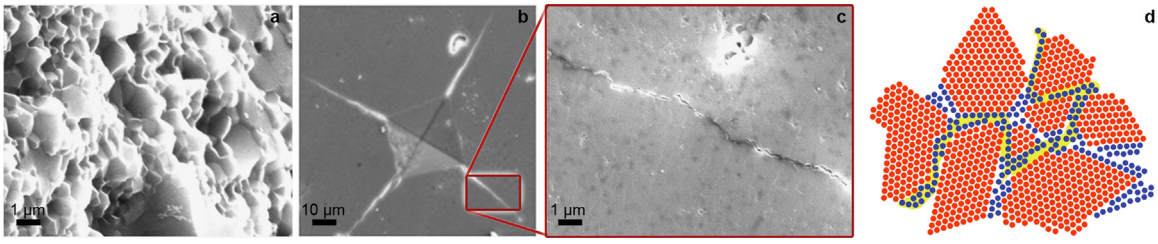

Fig. 4. Transgranular fracture in undoped HA (a) transforms into an intergranular mode in MgO-doped samples (b and c). As illustrated in (d) migration of MgO impurities (blue) to the grain boundaries confines growth of nanocracks to the intergranular space and therefore guides propagation of fracture through zigzag paths (yellow). Owing to this phenomenon while small amounts of MgO doping can improve fracture toughness without affecting other desirable attributes, excessive doping beyond 1 wt% may in contrast exacerbate other mechanical properties such as hardness and stiffness. (For interpretation of the references to color in this figure, the reader is referred to the web version of this article.)

of doping achieve a theoretical density of 95% and 98% at relatively low sintering temperatures of 1000 °C and 1050 °C respectively. For comparison majority of previous studies have reported only a relative density of ~75% at 1000 °C [14].

The improved fracture toughness observed in the present work could also be associated with the suppression of microcracks that would be present in the HA structure due to thermal expansion anisotropy (TEA) as reported by Hoepfner and Case [21]. According to these authors, such microcracks can be avoided if the mean grain size of the sintered HA is less than some critical grain size for microcracking due to TEA. In the present work, the MgO was found to be an effective grain growth inhibitor and as such it is expected that nanocrystalline grain size reduces the extent of micro-cracking resulting from TEA during the sintering of hydroxyapatite.

4. Conclusions

In summary we showed that mechanical properties of HA can be greatly influenced by preparation method and crystallinity of nanopowders. An optical wet chemical method can deliver remarkable improvements in terms of mechanical properties such as Young's modulus and Vickers hardness while further enhancement of fracture toughness can be achieved through minimal doping of samples by MgO. With exceptional biodurability of MgO-doped samples under simulated conditions, load bearing HA implants for clinical applications seem to be plausible through similar enhancements.

Acknowledgement

This study was supported under the HIR grant number H-16001–00-D000027. The authors gratefully acknowledge University of Malaya and the Ministry of Higher Education Malaysia for the financial support.

References

[1] B.L. Riggs, H.W. Wahner, W.L. Dunn, R.B. Mazess, K.P. Offord, KP, L.J. Melton, Differential changes in bone mineral density of the appendicular and axial skeleton with aging: relationship to spinal osteoporosis, Journal of Clinical Investigation 67 (1981) 328–335.

[2] P. Anagnostis, A. Karagiannis, K. Al Kakafika, V.G. Tziomalos, D.P. Athyros, Mikhailidis, Atherosclerosis and osteoporosis: age-dependent degenerative processes or related entities?, osteoporosis international 20 (2009) 197–207.

[3] M. Long, H. Rack, Titanium alloys in total joint replacement-a materials science perspective, Biomaterials 19 (1998) 1621–1639.

[4] T. Takaoka, M. Okumura, H. Ohgushi, K. Inoue, Y. Takakura, S. Tamai, Histological and biochemical evaluation of osteogenic response in porous hydroxyapatite coated alumina ceramics, Biomaterials 17 (1996) 1499–1505.

[5] R. Geesink, N. Hoefnagel, Six-year results of hydroxyapatite-coated total hip replacement., Journal of Bone And Joint Surgery British 77 (1995) 0534–547.

[6] X. Zheng, M. Huang, C. Ding, Bond strength of plasma-sprayed hydroxyapatite/Ti composite coatings, Biomaterials 21 (2000) 841–849.

[7] E. Morscher, A. Hefti, U. Aebi, Severe osteolysis after third-body wear due to hydroxyapatite particles from acetabular cup coating, Journal of Bone And Joint Surgery British 80 (1998) 267–272.

[8] M.K. Singh, T. Shokuhfar, J.J. dA Gracio, A.C.M. de Sousa, J.M.D.F. Fereira, H. Garmestani, S. Ahzi, Hydroxyapatite modified with carbon nanotube reinforced poly (methyl methacrylate): a nanocomposite material for biomedical applications, Advanced Functional Materials 18 (2008) 694–700.

[9] M.A. Lopes, F.J. Monteiro, J.D. Santos, Glass-reinforced hydroxyapatite composites: fracture toughness and hardness dependence on microstructural characteristics, Biomaterials 20 (1999) 2085–2090.

[10] E.S. Ahn, N.J. Gleason, A. Nakahira, J.Y. Ying, Nanostructure processing of hydroxyapatite based bioceramics, Nano Letters 1 (2001) 149–153.

[11] J.W. Choi, Y.M. Kong, H.E. Kim, I.S. Lee, Reinfocement of hydroxyapatite bioceramic by addition of Ni_3Al and Al_2O_3, Journal of the American Ceramics Society 81 (1998) 1743–1748.

[12] S.S. Banerjee, S. Tarafder, N.M. Davies, A. Bandyopadhyay, S. Bose, Understanding the influence of MgO and SrO binary doping on the mechanical and biological properties of β-TCP ceramics, Acta Biomaterialia 6 (2010) 4167–4174.

[13] H.S. Ryu, K.S. Hong, J.K. Lee, D.J. Kim, J.H. Lee, B.S. Chang, D.H. Lee, C.K. Lee, S.S. Chung, Magnesia-doped HA/β-TCP ceramics and evaluation of their biocompatibility, Biomaterials 25 (2004) 393–401.

[14] J. Elliott, P. Mackie, R. Young, Monoclinic Hydroxyapatite, Science 180 (1973) 1055–1057.

[15] M.G. Kutty, S. Ramesh, The effects of sintering temperature on the properties of hydroxyapatite, Cearmics International 26 (2000) 221–230.

[16] Y. Yang, E. Chang, S. Lee, Mechanical properties and Young's modulus of plasma-sprayed hydroxyapatite coating on Ti substrate in simulated body fluid, Journal of Biomedical Materials Research Part A 67 (2003) 886–899.

[17] E. Landi, S. Sprio, M. Sandri, G. Celotti, A. Tampieri, Development of Sr and CO_3 cosubstituted hydroxyapatites for biomedical applications, Acta Biomaterialia 4 (2008) 656–663.

[18] H. Morgan, R. Wilson, J. Elliott, S. Dowker, P. Anderson, Preparation and characterisation of monoclinic hydroxyapatite and its precipitated carbonate apatite intermediate, Biomaterials 21 (2000) 617–627.

[19] A. Jillavenkatesa, R. Condrate Sr, Sol–gel processing of hydroxyapatite, Journal of Material Science 33 (1998) 4111–4119.

[20] E. Landi, A. Tampieri, G. Celotti, S. Sprio, Densification behaviour and mechanisms of synthetic hydroxyapatites, Jouurnal of European Ceramics Society 20 (2000) 2377–2387.

[21] T.P. Hoepfner, E.D. Case, An estimate of the critical grain size for microcracks induced in hydroxyapatite by thermal expansion anisotropy, Matterial Letters 58 (2004) 489–492.